J|A|C|S
ARTICLES

Published on Web 04/05/2008

Self-Assembled Zinc Chlorin Rod Antennae Powered by Peripheral Light-Harvesting Chromophores

Cornelia Röger,[†] Yuliya Miloslavina,[‡] Doris Brunner,[†] Alfred R. Holzwarth,*[,‡] and Frank Würthner*[,†]

Contribution from the Universität Würzburg, Institut für Organische Chemie and Röntgen Research Center for Complex Material Systems, Am Hubland, D-97074 Würzburg, Germany, and Max-Planck-Institut für Bioanorganische Chemie, Postfach 101365, D-45470 Mülheim an der Ruhr, Germany

Received November 12, 2007; E-mail: wuerthner@chemie.uni-wuerzburg.de; holzwarth@mpi-muelheim.mpg.de

Abstract: The multichromophoric dyads **1**, **2** and triad **3** have been synthesized by coupling of the appropriately functionalized chlorin derivative with naphthalene diimide dyes through esterification, and subsequent metalation of the chlorin center with zinc acetate. The self-assembly properties of naphthalene diimide (NDI)-zinc chlorin (ZnChl) dyads **1**, **2** and triad **3** have been studied in nonpolar, aprotic solvents by UV–vis, CD, and steady-state emission spectroscopy, revealing formation of rod-like structures by noncovalent interactions of zinc chlorin units, while the appended naphthalene diimide dyes do not aggregate at the periphery of the rod antennae. In all these systems, photoexcitation of the enveloping naphthalene diimides at 540 and 620 nm, respectively, leads to highly efficient energy-transfer processes (FRET; $\phi_{ET} \geq 0.99$) to the inner zinc chlorin backbone, as explored by time-resolved fluorescence spectroscopy on the picosecond time scale. The efficiencies of zinc chlorin rod aggregates for the harvesting of solar light are markedly increased from 26% for dyad **2** up to 63% for triad **3**, compared to the LH capacity of the monochromophoric aggregates of model system ZnChl **6a**. Thus, with the self-assembled zinc chlorin rod antenna based on triad **3**, a highly efficient artificial LH system has been achieved.

Introduction

In most of natural photosynthetic light-harvesting (LH) complexes, sunlight is collected not only by chlorophyll (Chl) or bacteriochlorophyll (BChl) chromophores, which are powerful absorbers in the violet, blue, and red wavelength regions, but also by accessory LH dyes such as phycobilines and carotenoids to make use of the intensive green region of the solar spectrum. In the majority of LH complexes, all the chromophores are embedded in a rigid protein scaffold, providing a sophisticated geometrical arrangement in order to guarantee efficient excitation energy transport within the LH system.[1] As an exception, the LH complexes of green photosynthetic bacteria and of the green filamentous bacterium *Chloroflexus aurantiacus*, the so-called chlorosomes, do not contain such a variety of LH chromophores since they lack a protein matrix to maintain a diverse constitution.[2] Chlorosomes show flattened sac-like structures which mainly include, besides a few carotenoids, cylindrical self-assemblies of BChl *c*, *d*, and *e* whose defined arrangement is imparted merely by intermolecular forces between the BChl molecules.[2,3] However, chlorosomes take advantage of their spartan constitution, since the tight packing of BChls within the self-assembled rods provides a high chromophore density and affords a large cross section for red/NIR light absorption. Therefore, it is not surprising that the most extremely low-sunlight-adapted phototrophic system known to date is a population of green sulfur bacteria inhabiting the Black Sea chemocline at depths of 100 m.[4] Recently, another green sulfur bacterial species was found to inhabit a deep-sea hydrothermal vent at depths of even 2300 m, where the only source of light is geothermal radiation.[5]

In recent years, it has been demonstrated that the self-assembly process of BChl *c*, *d*, and *e* into rod-like structures can be achieved, not only *in vivo* but also *in vitro*, by choosing nonpolar, aprotic solvents.[3a,6] Zinc chlorins (ZnChl), which are readily available by stepwise derivatization of Chl *a*, serve as appropriate model compounds for natural BChl by performing

[†] Universität Würzburg.
[‡] Max-Planck-Institut für Bioanorganische Chemie, Mülheim an der Ruhr.

(1) (a) *Photosynthetic Light-Harvesting Systems: Organization and Function*; Scheer, H.; Schneider, S., Eds.; de Gruyter: Berlin, 1988. (b) Huber, R. *Biosci. Rep.* **1989**, *9*, 635–73. (c) Katz, J. *J. Photosynth. Res.* **1990**, *26*, 143–160. (d) Cogdell, R. J.; Lindsay, J. G. *New Phytol.* **2000**, *145*, 167–196. (e) Holzwarth, A. R. In *Series on Photoconversion of Solar Energy*; Archer, M. D., Barber, J., Eds.; Imperial College Press: London, U.K., 2002; pp 43–115. (f) Scholes, G. D.; Fleming, G. R. *Adv. Chem. Phys.* **2006**, *132*, 57–129.
(2) Olson, J. M. *Photochem. Photobiol.* **1998**, *67*, 61–75.
(3) (a) Balaban, T. S.; Tamiaki, H.; Holzwarth, A. R. *Top. Curr. Chem.* **2005**, *258*, 1–38. (b) Holzwarth, A. R.; Schaffner, K. *Photosynth. Res.* **1994**, *41*, 225–233.
(4) Manske, A. K.; Glaeser, J.; Kuypers, M. M. M.; Overmann, J. *Appl. Environ. Microbiol.* **2005**, *71*, 8049–8060.
(5) Beatty, J. T.; Overmann, J.; Lince, M. T.; Manske, A. K.; Lang, A. S.; Blankenship, R. E.; Van Dover, C. L.; Martinson, T. A.; Plumley, F. G. *Proc. Natl. Acad. Sci. U.S.A.* **2005**, *102*, 9306–9310.
(6) (a) Bystrova, M. I.; Mal'gosheva, I. N.; Krasnovsky, A. A. *Mol. Biol. (Moscow)* **1979**, *13*, 440–451. (b) Staehelin, L. A.; Golecki, J. R.; Drews, G. *Biochim. Biophys. Acta* **1980**, *589*, 30–45. (c) Smith, K. M.; Kehres, L. A. *J. Am. Chem. Soc.* **1983**, *105*, 1387–1389. (d) Worcester, D. L.; Michalski, T. J.; Katz, J. J. *Proc. Natl. Acad. Sci. U.S.A.* **1986**, *83*, 3791–3795.

 © 2008 American Chemical Society

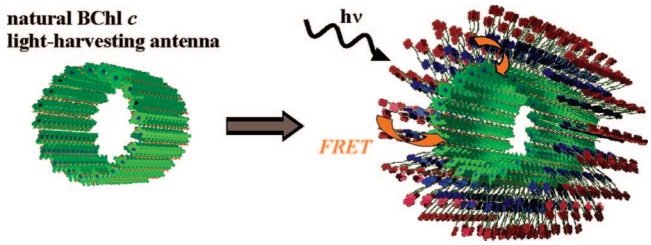

Figure 1. Concept for the improvement of natural BChl *c* LH antennae by means of additional peripheral red and blue chromophores that harvest the green and orange fraction of solar light. FRET denotes "Förster Resonance Energy Transfer".

an analogous self-assembly process into rod-like structures.[3a,7] BChl and ZnChl self-assemblies have drawn considerable attention as they show very high exciton mobilities,[8] which make these aggregates potentially interesting for applications in supramolecular photonic and electronic devices. A decisive advancement toward the preparation of well-defined nanorods for the development of materials based on artificial ZnChl LH systems was achieved by functionalization of ZnChl monomers with solubilizing alkyl chains, leading to well-soluble self-assembled ZnChl nanorods.[9]

However, for an application of such supramolecular systems in light harvesting and photovoltaics, not only well-defined nanostructures but also optimal utilization of the terrestrial solar spectrum is required.[10] Since ZnChl aggregates are not well-suited for absorption of the dominant green and orange regions of solar irradiance due to the above-mentioned lack of appropriate absorption bands, we intended to design multichromophoric LH systems consisting of the cylindrical ZnChl antenna and additional light-absorbing LH chromophores in the periphery of the nanorod (Figure 1).

In a recent communication, we have demonstrated on the basis of naphthalene diimide-zinc chlorin dyad **2** (Chart 1) that the concept depicted in Figure 1 is indeed viable.[11] We have chosen 2,6-core-disubstituted naphthalene diimides (NDIs) as additional LH chromophores, because the absorption maxima of these strong and photostable fluorophores can be easily tuned within the whole range of the "green gap" by variation of the electron-donating character of the core substituents.[12] We have now extended our novel concept to the newly developed triad ZnChl-NDI_{NN}-NDI_{NO} **3** and synthesized the new dyad **1** (Chart 1) and thoroughly investigated the self-assembly behavior of these multichromophoric conjugates as well as energy-transfer processes in their monomers and aggregates.

Results and Discussion

Synthesis of Dyad ZnChl-NDI_{NO} 1 and Triad ZnChl-NDI_{NN}-NDI_{NO} 3. The dyad ZnChl-NDI_{NO} **1** was synthesized according to the route outlined in Scheme 1. Chlorin propionic acid **10**, which is a key compound for the synthesis of ZnChl-NDI conjugates, was obtained by stepwise derivatization of natural Chlorophyll (Chl) *a*,[7c,13] the latter of which was extracted from the cyano bacterium *Spirulina platensis*.[13a] The precursor of all 2,6-core-disubstituted NDI dyes used in this work, namely *N*,*N*′-bis-(2′,6′-diisopropylphenyl)-2,6-dichloronaphthalene-1,4,5,8-tetracarboxylic acid diimide, was prepared by stepwise transformations of pyrene as reported previously.[12c] Nucleophilic substitution of one chlorine atom of the 2,6-dichloro-core-substituted NDI with 6-hydroxyhexylamine according to literature provided the starting material NDI **7**.[11]

The hydoxy group of NDI **7** was protected by reaction with *tert*-butyldiphenylsilyl chloride to afford NDI **8** quantitatively (Scheme 1, step i). In the next step, the remaining chlorine atom was replaced by nucleophilic substitution with 1,6-hexanediol in the presence of potassium carbonate, followed by esterification of the newly introduced hydroxy group with 3,5-bis(dodecyloxy)benzoic acid (step ii). Cleavage of the silyl protecting group with TBAF gave the pink NDI_{NO} **4** (step iii; for structure, see Chart 1). The esterification of chlorin propionic acid **10** with the hydroxyl-functionalized NDI_{NO} **4** by using DCC, DMAP, and DPTS in the presence of *N*-ethyldiisopropylamine gave the precursor **11** (step iv). Selective reduction of the aldehyde group of compound **11** was achieved with borane-*tert*-butylamine complex, and the central zinc ion in chlorin was introduced by metalation in the presence of saturated methanolic zinc acetate solution to afford the hitherto unknown dyad ZnChl-NDI_{NO} **1**. Dyad **2** was prepared by a similar route as reported before.[11]

The synthetic route to triad **3** is outlined in Scheme 2 that starts from NDIs **12** and **16**; the latter dyes were synthesized according to literature.[12a] The amino functionality of NDI **12** was protected by a *tert*-butylcarbonyl (BOC) group, followed by substitution of the chlorine atom with 1,6-hexanediol, esterification with 3,5-bis(dodecyloxy)benzoic acid, and cleavage of the BOC group to yield the pink colored NDI building block **15** (steps i−iii). The blue-colored NDI building block **17** was synthesized from NDI **16** by nucleophilic substitution with 6-hydroxyhexylamine (step iv). Coupling of amine **15** with carboxylic acid **17** in the presence of HATU gave NDI_{NN}-NDI_{NO} **18** (step v) which was subsequently esterified with chlorin propionic acid **10** to obtain compound **19** (step vi). Reduction of the aldehyde group in the latter compound and subsequent metalation of the chlorin center with zinc acetate (step vii) finally afforded the desired triad ZnChl-NDI_{NN}-NDI_{NO} **3**.

(7) (a) Tamiaki, H.; Holzwarth, A. R.; Schaffner, K. *J. Photochem. Photobiol. B* **1992**, *15*, 355–360. (b) Cheng, P.; Lidell, P. A.; Ma, S. X. C.; Blankenship, R. E. *Photochem. Photobiol.* **1993**, *58*, 290–295. (c) Tamiaki, H.; Amakawa, M.; Shimono, Y.; Tanikaga, R.; Holzwarth, A. R.; Schaffner, K. *Photochem. Photobiol.* **1996**, *63*, 92–99. (d) Hildebrandt, P.; Tamiaki, H.; Holzwarth, A. R.; Schaffner, K. *J. Phys. Chem.* **1994**, *98*, 2191–2197.

(8) (a) Prokhorenko, V. I.; Steensgard, D. B.; Holzwarth, A. R. *Biophys. J.* **2000**, *79*, 2105–2120. (b) Prokhorenko, V. I.; Holzwarth, A. R.; Müller, M. G.; Schaffner, K.; Miyatake, T.; Tamiaki, H. *J. Phys. Chem. B* **2002**, *106*, 5761–5768. (c) Psencik, J.; Ma, Y.-Z.; Arellano, J. B.; Hála, J.; Gillbro, T. *Biophys. J.* **2003**, *84*, 1161–1179.

(9) Huber, V.; Katterle, M.; Lysetska, M.; Würthner, F. *Angew. Chem., Int. Ed.* **2005**, *44*, 3147–3151.

(10) (a) For reviews on supramolecular LH systems, see: Balzani, V.; Ceroni, P.; Maestri, M.; Vicinelli, V. *Curr. Opin. Chem. Biol.* **2003**, *7*, 657–665. (b) Fréchet, J. M. J. *J. Polym. Sci., Polym. Chem. Ed.* **2003**, *41*, 3713–3725. (c) Würthner, F. *Chem. Commun.* **2004**, 1564–1579. (d) Hoeben, F. J. M.; Jonkheim, P.; Meijer, E. W.; Schenning, A. P. H. J. *Chem. Rev.* **2005**, *105*, 1491–1546. (e) Wasielewski, M. R. *J. Org. Chem.* **2006**, *71*, 5051–5066. (f) For recent articles on multichromophoric supramolecular nanorods, see: Yamamoto, Y.; Fukushima, T.; Suna, Y.; Ishii, N.; Saeki, A.; Seki, S.; Tagawa, S.; Taniguchi, M.; Kawai, T.; Aida, T. *Science* **2006**, *314*, 1761–1764. (g) Miller, R. A.; Presley, A. D.; Francis, M. B. *J. Am. Chem. Soc.* **2007**, *129*, 3104–3109.

(11) Röger, C.; Müller, M. G.; Lysetska, M.; Miloslavina, Y.; Holzwarth, A. R.; Würthner, F. *J. Am. Chem. Soc.* **2006**, *128*, 6542–6543.

(12) (a) Würthner, F.; Ahmed, S.; Thalacker, C.; Debaerdemaeker, T. *Chem.—Eur. J.* **2002**, *8*, 4742–4750. (b) Thalacker, C.; Miura, A.; De Feyter, S.; De Schryver, F. C.; Würthner, F. *Org. Biomol. Chem.* **2005**, *3*, 414–422. (c) Thalacker, C.; Röger, C.; Würthner, F. *J. Org. Chem.* **2006**, *71*, 8098–8105.

(13) (a) Smith, K. M.; Goff, D. A.; Simpson, D. J. *J. Am. Chem. Soc.* **1985**, *107*, 4946–4954. (b) Kosaka, N.; Tamiaki, H. *Eur. J. Org. Chem.* **2004**, *11*, 2325–2330.

Chart 1. Chemical Structures of ZnChl-NDI_{NO} **1**, ZnChl-NDI_{NN} **2**, ZnChl-NDI_{NN}-NDI_{NO} **3**, and Reference Chromophores **4**–**6**[a]

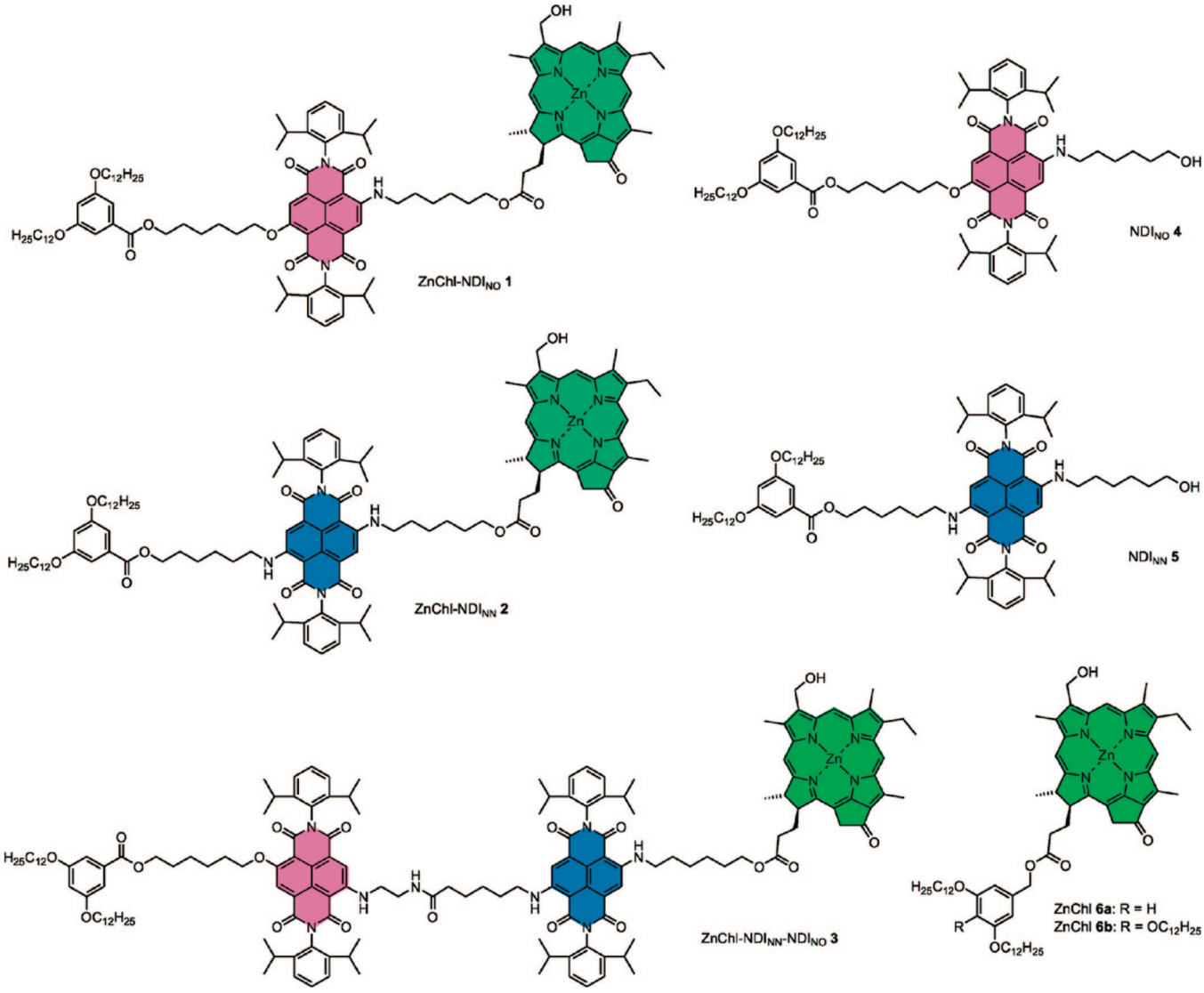

[a] NN and NO in compound codes donate "nitrogen, nitrogen" and "nitrogen, oxygen" substituents, respectively, at the 2,6-positions of naphthalene diimide (NDI) unites.

The new dyad **1** and triad **3** are properly characterized by ^{1}H NMR and UV–vis spectroscopy and high resolution mass spectrometry. The detailed synthetic procedures and characterization data, also for the key unknown intermediates, are given in the Supporting Information.

Steady-State Spectral Properties of Dyads 1 and 2 Monomers and their Aggregates. One of the most characteristic features of BChl *c*, *d*, *e* and related ZnChl dyes is that they form J-aggregates with a pronounced bathochromic shift of the S_0-S_1 transition band, namely the Q_y-band, of about 80–90 nm compared to the respective monomer spectra.[7,9,13] The formation of such aggregates was observed in water, or in nonpolar aprotic solvents such as *n*-hexane or cyclohexane already at a low concentration ($\sim 10^{-6}$ M) owing to the interplay of three different types of noncovalent interactions between the molecular building blocks.[7,9] The combination of $\pi-\pi$ stacking of the extended aromatic core and coordination of the 3^1 hydroxy group to the central metal ion of a neighboring molecule leads to the formation of one-dimensional chromophore stacks.[14] These stacks are held together by hydrogen bonding between the 3^1 hydoxy group and the 13^1 keto functionality, resulting in rod-like supramolecular structures.[6d,7d,8a,9] In Figure 2, such a typical rod aggregate absorption spectrum is depicted for ZnChl **6a** (green line). In contrast, the absorption and emission spectra of the additional antenna chromophores used in this work, namely NDI_{NO} **4** (pink line) and NDI_{NN} **5** (blue line), in cyclohexane/tetrachloromethane (1%) exhibit the characteristic shapes and maxima of 2,6-core-substituted NDI monomers, respectively.[12] This observation can be explained in terms of the bulky 2,6-diisopropylphenyl imide substituents that prevent NDIs **4** and **5** from intermolecular $\pi-\pi$ interactions.

To explore the self-assembly behavior of multichromophoric dyads **1** and **2**, UV–vis spectra were recorded in the polar solvent tetrahydrofuran (THF) and in the nonpolar solvent mixture cyclohexane/tetrachloromethane (1%). Figure 3 shows the UV–vis absorption and normalized fluorescence spectra of dyads **1** and **2**. If THF was used as a solvent, UV–vis spectra of both dyads **1** and **2** revealed the characteristic Q_y-band of ZnChl monomers[7,9] (λ_{max} = 647 and 646 nm, respectively), since in this solvent metal ion coordination and hydrogen bonding

(14) Huber, V.; Lysetska, M.; Würthner, F. *Small* **2007**, *3*, 1007–1014.

Scheme 1. Synthesis of ZnChl-NDI$_{NO}$ **1**[a]

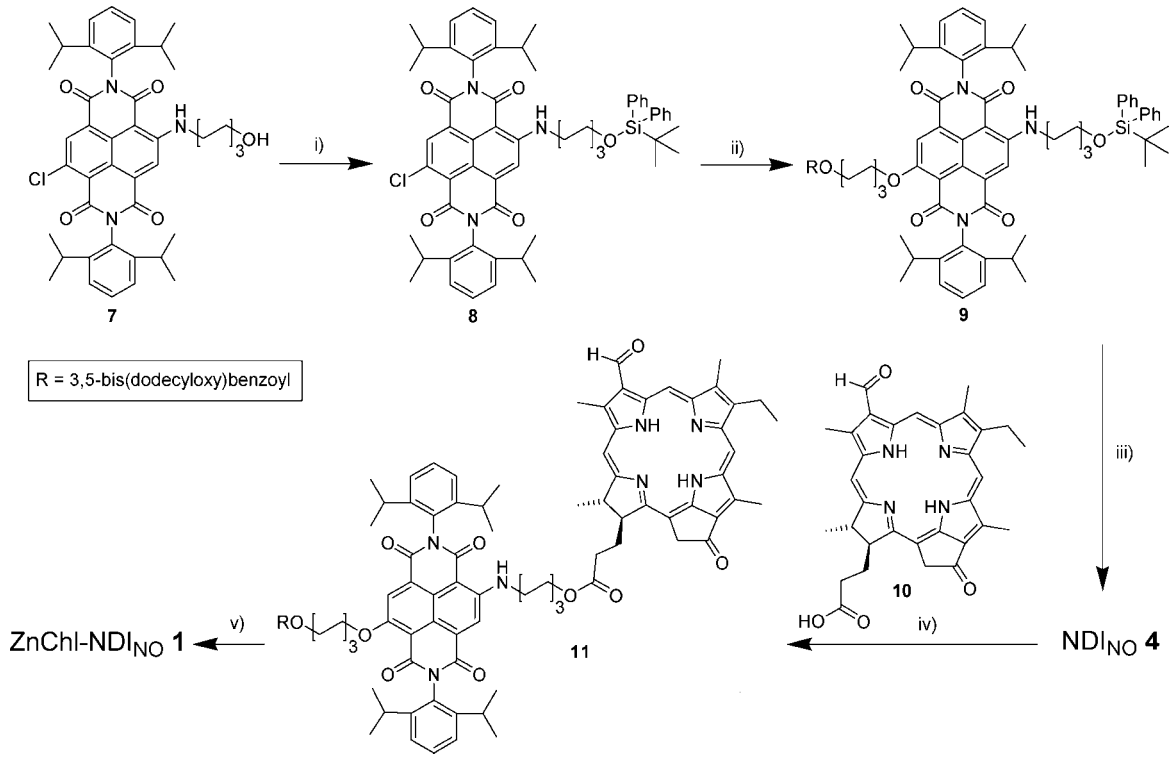

[a] Reagents and conditions: (i) *tert*-Butyldiphenylsilyl chloride, imidazol, DMAP, CH_2Cl_2, rt, 30 min, >99% of **8**; (ii) 1,6-hexanediol, K_2CO_3, 100 °C, 12 h; 3,5-bis(dodecyloxy)benzoic acid, DCC, DMAP, DPTS, CH_2Cl_2, rt, 3 h, 68% of **9**; (iii) tetra-*n*-butylammonium fluoride (TBAF), THF, rt, 4 h, 64% of **4**; (iv) DCC, DMAP, DPTS, *N*-ethyldiisopropylamine, CH_2Cl_2, Ar, rt, 24 h, 39% of **11**; (v) BH_3(*t*-$BuNH_2$), CH_2Cl_2, 0 °C, 3 h; $Zn(OAc)_2 \times 2H_2O$, MeOH, THF, rt, 6 h, 50% of ZnChl-NDI **1**. DCC = dicyclohexylcarbodiimide, DMAP = 4-(dimethylamino)pyridine, DPTS = 4-(dimethylamino)pyridinium 4-toluenesulfonate.

between ZnChl units are prevented due to the ligation of THF as a fifth ligand at the zinc ion and its hydrogen-bond acceptor ability. The absorption maxima of the respective NDI units are located in the "green gap" of the ZnChl absorption spectrum (λ_{max} = 550 nm for **1** and 607 nm for **2**, respectively). Both of the NDI absorption bands match the UV–vis spectra of the individual NDI chromophores **4** (λ_{max} = 547 nm, THF) and **5** (λ_{max} = 614 nm, THF), respectively, indicating that there are no ground-state interactions between NDI and monomeric ZnChl units.

The fluorescence spectra of **1** and **2** monomers do not exhibit any NDI emission bands, although NDI reference components **4** and **5** are highly fluorescent (ϕ_{Fl} = 0.58 and 0.39, respectively, in THF). Likewise, the fluorescence quantum yields of dyad **1** and **2** monomers (ϕ_{Fl} = 0.12 and 0.11, respectively), which were determined by selective excitation of the respective NDI S_0-S_1 absorption band, are in the same range as the quantum yield of ZnChl **6a** monomers (ϕ_{Fl} = 0.19, in THF), suggesting almost complete quenching of NDI emission by the appended ZnChl chromophore.

In the nonpolar aprotic solvent system cyclohexane/tetrachloromethane (1%), good solubility for dyads **1** and **2** is given, despite the fact that the fifth coordination site of the zinc ion and the hydroxyl functionality are not well solvated. As a consequence, self-assembly into J-aggregates takes place for these dyads in this solvent system as revealed by a bathochromic shift of the ZnChl Q_y-band to 729 and 731 nm, respectively (see Figure 3). It is noticed that the absorption spectra of NDI units in **1** and **2** aggregates (λ_{max} = 545 and 611 nm, respectively) are only slightly bathochromically shifted compared to those of the isolated NDI chromophores **4** and **5** (λ_{max} = 540 and 604 nm, respectively, Figure 2). This observation suggests that in aggregates of dyads **1** and **2** no excitonic coupling between NDI units occurs.

Further evidence for the J-type excitonic coupling of ZnChl units of **1** and **2** in cyclohexane/tetrachloromethane (1%) is provided by steady-state fluorescence spectra (Figure 3). Aggregated species of **1** and **2** show a very small Stokes shift of the ZnChl Q_y-band ($\Delta\lambda$ = 8 and 6 nm, respectively), which is characteristic for BChl and ZnChl J-aggregates, signifying thermal equilibration of the Q_y excitonic states.[2] Moreover, for aggregates of **1** and **2**, complete quenching of the fluorescence of the respective NDI units is observed, and the quantum yields of the emission from the ZnChl subunits have decreased to $\phi_{Fl} \leq 0.001$. These results imply that not only the emission of the NDI units is quenched but also the aggregated ZnChl species is poorly fluorescent. Such low fluorescence quantum yields are characteristic for ZnChl and BChl *c*, *d*, *e* aggregates, since efficient quenching processes originate from the presence of small amounts of oxidized chlorin,[8b] which cannot be excluded for the present system. However, it had been demonstrated for both chlorosomes and artificial chlorin aggregates that their LH efficiencies are not adversely affected by these quenching processes if effective energy acceptors are present.[8b,15] For instance, in chlorosomes the excitation energy of the rod

(15) (a) Brune, D. C.; King, G. H.; Infosino, A.; Steiner, T.; Thewalt, M. L. W.; Blankenship, R. E. *Biochemistry* **1987**, *26*, 8652–8658. (b) Holzwarth, A. R.; Griebenow, K.; Schaffner, K. *J. Photochem. Photobiol. A: Chem.* **1992**, *65*, 61–71. (c) Savikhin, S.; Zhu, Y.; Blankenship, R. E.; Struve, W. S. *J. Phys. Chem.* **1996**, *100*, 3320–3322. (d) Miyatake, T.; Tamiaki, H.; Holzwarth, A. R.; Schaffner, K. *Helv. Chim. Acta* **1999**, *82*, 797–810.

Scheme 2. Synthesis of ZnChl-NDI_{NN}-NDI_{NO} **3**[a]

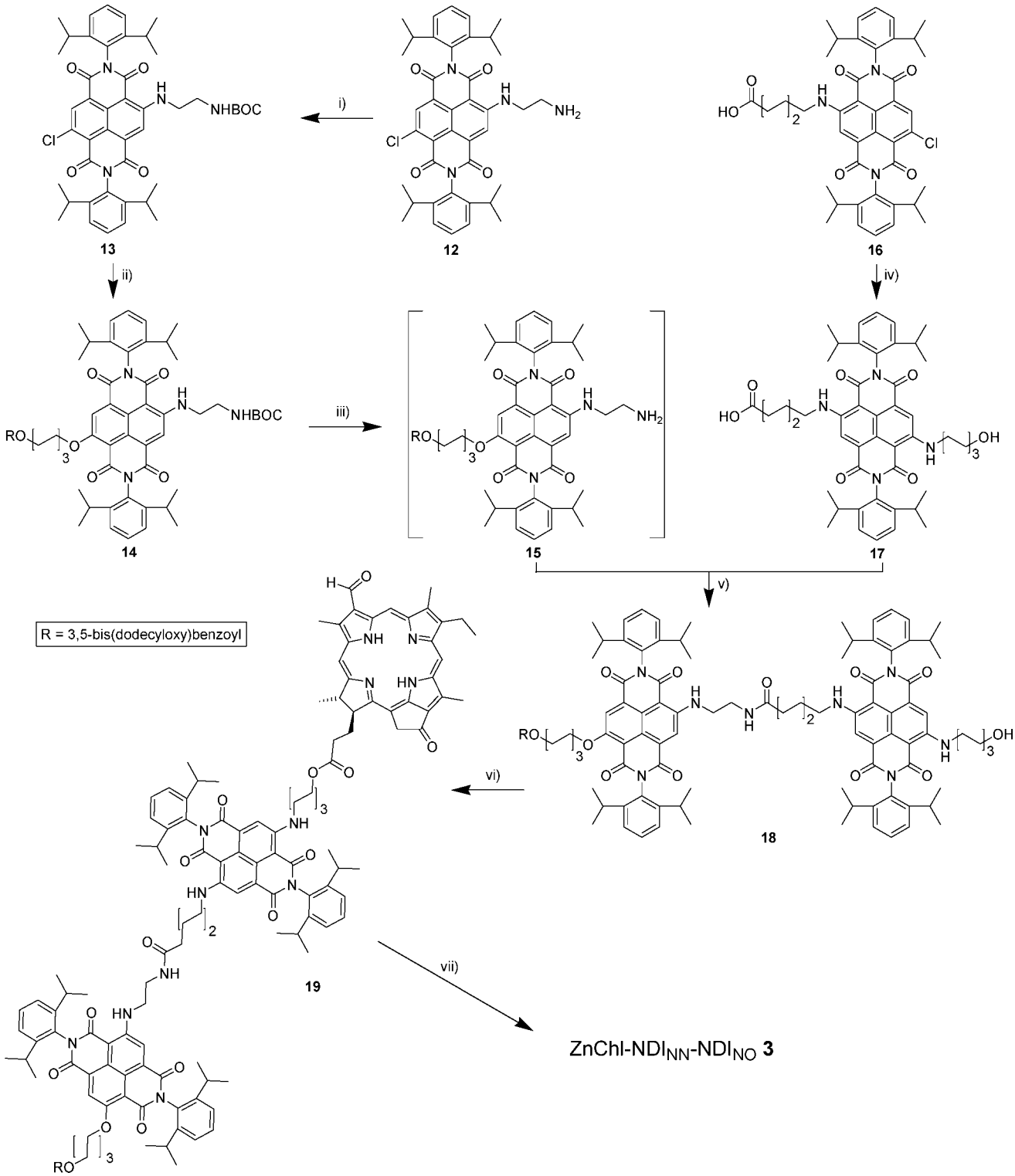

[a] Reagents and conditions: (i) BOC_2O, CH_2Cl_2, rt, 30 min, 87% of **13**; (ii) 1,6-hexanediol, K_2CO_3, 80 °C, 6 h; 3,5-bis(dodecyloxy)benzoic acid, DCC, DMAP, DPTS, CH_2Cl_2, rt, 3 h, 55% of **14**; (iii) CF_3COOH, CH_2Cl_2, rt, 30 min, 97% of **15**; (iv) 6-aminohexanol, 80 °C, 2 h, 91% of **17**; (v) HATU, *N*-ethyldiisopropylamine, CH_2Cl_2, rt, 5 min, 62% of **18**; (vi) chlorin propionic acid **10**, DCC, DMAP, DPTS, *N*-ethyldiisopropylamine, CH_2Cl_2, Ar, 35 °C, 24 h, 26% of **19**; (vii) BH_3(*t*-$BuNH_2$), CH_2Cl_2, 0 °C, 3 h; $Zn(OAc)_2 \times 2H_2O$, MeOH, THF, rt, 16 h, 66% of ZnChl-NDI_{NN}-NDI_{NO} **3**. HATU = *O*-(7-azabenzotriazole-1-yl)-*N*,*N*,*N*′,*N*′-tetramethyluronium hexafluorophosphate.

antennae is transferred efficiently to BChl *a* protein complexes in the so-called baseplate,[15a–c] while for artificial ZnChl LH systems coaggregated BChl *a* functionalities work as efficient energy acceptors.[15d]

To further elaborate the aggregation process of ZnChl-NDI dyads **1** and **2**, temperature-dependent UV–vis spectroscopic measurements were carried out in cyclohexane/tetrachloromethane (1%). Figure 4A shows the temperature-dependent

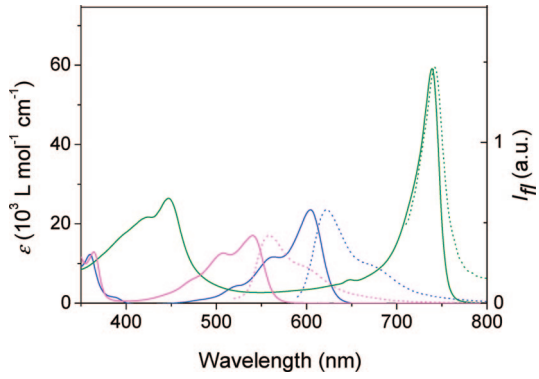

Figure 2. UV–vis (solid lines) and normalized fluorescence spectra (dotted lines) of ZnChl **6a** rod aggregate in cyclohexane/tetrachloromethane (1%)/THF (0.1%) (green lines, λ_{ex} = 700 nm), NDI_{NO} **4** in cyclohexane/tetrachloromethane (1%) (pink lines, λ_{ex} = 510 nm), and NDI_{NN} **5** in cyclohexane/tetrachloromethane (1%) (blue lines, λ_{ex} = 575 nm).

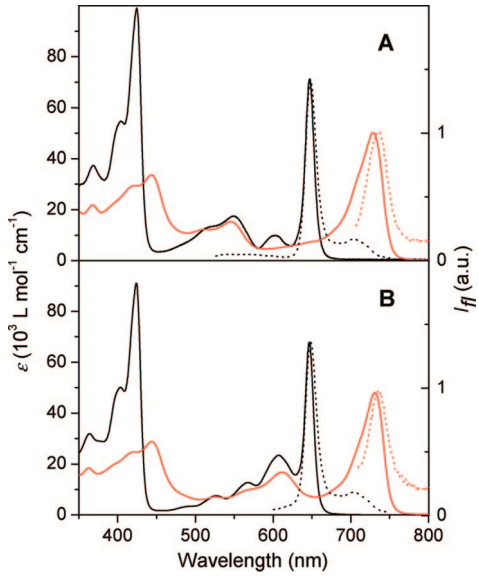

Figure 3. (A) UV–vis (solid lines) and normalized fluorescence (dashed lines, λ_{ex} = 510 nm) spectra of **1**. Monomers in THF (black); aggregates in cyclohexane/tetrachloromethane (1%) (red) at room temperature. (B) UV–vis (solid lines) and normalized fluorescence (dashed lines, λ_{ex} = 530 nm) spectra of **2**. Monomers in THF (black); aggregates in cyclohexane/tetrachloromethane (1%) (red) at room temperature.

absorption spectra of a solution of dyad **1** which was first heated to 65 °C. After a 1 h equilibration time, the UV–vis spectrum revealed not only a strongly decreased aggregate absorption band at 729 nm but also an absorption maximum at 646 nm, indicating a risen amount of monomers of **1** in the equilibrium at this temperature. On subsequent cooling of the sample from 65 to 25 °C in 10 °C intervals and an equilibration time of again 1 h, the Q_y-band of aggregates regained its initial intensity, while the monomer band disappears completely, confirming the reversibility of aggregate formation. As shown in the inset of Figure 4A, the absorption versus temperature plot provides a sigmoidal curve with a melting temperature of about 64 °C for the aggregates in the solvent system applied. Thus, the temperature dependence of monomer−aggregate equilibria of dyad **1** properly resembles the characteristics of dyad **2**.[11]

The self-assembly process of ZnChl dyes such as ZnChls **6** into cylindrical structures goes along with an induced circular dichroism (CD) effect due to excitonic coupling, as the transition dipole moments of chiral ZnChls are arranged helically.[16] Examination of an aggregate solution of ZnChl-NDI_{NO} **1** in cyclohexane/tetrachloromethane (1%) by CD spectroscopy reveals such a Cotton effect for the chlorin Q_y absorption band as well (Figure 4B). The displayed effect consists of an exciton couplet, whose shape resembles the signals observed previously for aggregates of ZnChls **6**.[9] By contrast, no Cotton effect of the peripheral NDI_{NO} units could be detected; thus, these chromophores do not interact with each other in the self-assembled dyad **1** which corroborates the results of UV–vis spectroscopy. After increasing the temperature of the aggregate solution of **1** to 65 °C and an equilibration time of 1 h, the intensity of the induced CD effect is diminished, indicating dissolution of the aggregated species into monomers. On stepwise decrease of the temperature to 25 °C in intervals of 10 °C and equilibration times of 1 h, the amplitude of the exciton couplet rises again. This increase can be taken as further evidence for the reversibility of the aggregation process of dyad **1** in cyclohexane/tetrachloromethane (1%). Temperature-dependent CD spectroscopy of dyad **2** aggregates revealed similar aggregation behavior as observed for dyad **1**(see Figure S1 in the Supporting Information).

Steady-State Spectral Properties and Aggregation Process of Triad 3. The absorption spectrum of triad **3** in THF exhibits the absorption maxima of the two different NDI components at 552 and 610 nm, respectively, along with the typical ZnChl monomer Q_y-band at 647 nm (Figure 5A). In cyclohexane/tetrachloromethane (1%) the characteristic bathochromic shift of the Q_y-band to 731 nm signifies J-type excitonic coupling of the ZnChl units in a similar manner as observed for dyads **1** and **2** (λ_{max} = 729 and 731 nm, respectively). Importantly, the "green gap" of ZnChl absorption is now effectively covered by the absorption bands of the NDI_{NO} and NDI_{NN} units, whose absorption maxima (λ_{max} = 551 and 619 nm, respectively) are only slightly shifted compared to those of the NDI_{NN}-NDI_{NO} component **18** (λ_{max} = 543 and 612 nm), indicating that there are no significant interactions between peripheral NDI chromophores within the self-assembly of triad **3**. This result is further supported by the CD spectrum of **3** aggregates (Figure 5B), which shows the characteristic bisignate Cotton effect resembling the exciton couplet of **1** and **2** aggregates (Figure 4B and Figure S1), but lacks any signal originating from the NDI units.

Stationary fluorescence spectra of **3** monomers that have been measured at the selective excitation of either the NDI_{NN} or NDI_{NO} unit only reveal an emission band originating from the Q_y-band of ZnChl (λ_{max} = 648 and 704 nm), while the emission of both NDI chromophores is completely quenched. The fluorescence quantum yield of **3** monomers (ϕ_{Fl} = 0.11) is independent of the excitation wavelength and resembles the values obtained for **1**, **2**, and **6a** monomers.

Aggregates of **3** show a small Stokes shift ($\Delta\lambda$ = 4 nm) and are only slightly fluorescent, since the emission of both NDI units is quenched again by the ZnChl aggregate. Moreover, the emission spectrum of dyad **18** that was recorded at a selective excitation of the pink NDI_{NO} unit (λ_{ex} = 520 nm) resembles exclusively the emission spectrum of NDI_{NN}, indicating efficient energy transfer from NDI_{NO} to the blue NDI_{NN} building block.

On the basis of the results obtained from steady-state studies on ZnChl-NDI conjugates **1**−**3**, one can reasonably draw the

(16) (a) Berova, N.; Nakanishi, K. In *Circular Dichroism: Principles and Applications*; Berova, N., Nakanishi, K., Woody, R., Eds.; VCH: New York, 2000; pp 337–368. (b) Prokhorenko, V. I.; Steensgaard, D. B.; Holzwarth, A. R. *Biophys. J.* **2003**, *85*, 3173–3186.

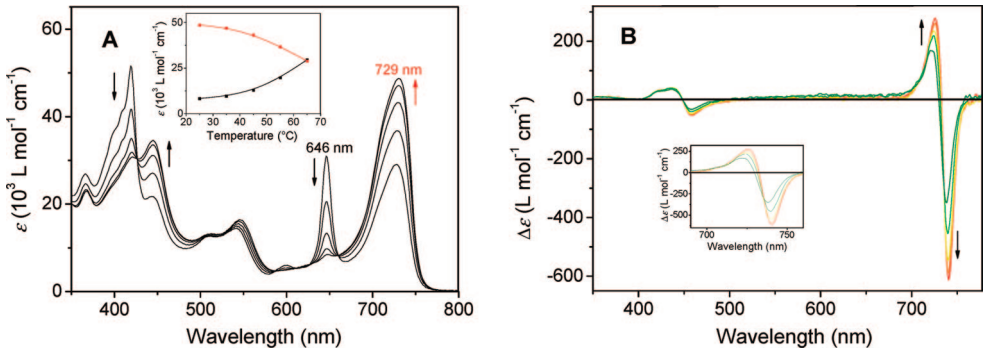

Figure 4. Temperature-dependent (A) UV–vis ($c = 2.5 \times 10^{-6}$ M) and (B) CD ($c = 3.0 \times 10^{-6}$ M) spectra of ZnChl-NDI_{NO} **1** in cyclohexane/tetrachloromethane (1%). The initial temperature of 65 °C was successively decreased to 25 °C in 10 °C steps, and at each temperature the solution was equilibrated for 1 h; the arrows indicate the changes upon decreasing temperature. Inset in (A): Increase of the Q_y-band of aggregates at 729 nm (red) and the decrease of the monomer band at 646 nm (black) upon decreasing temperature. Inset in (B): Magnification of the CD signals.

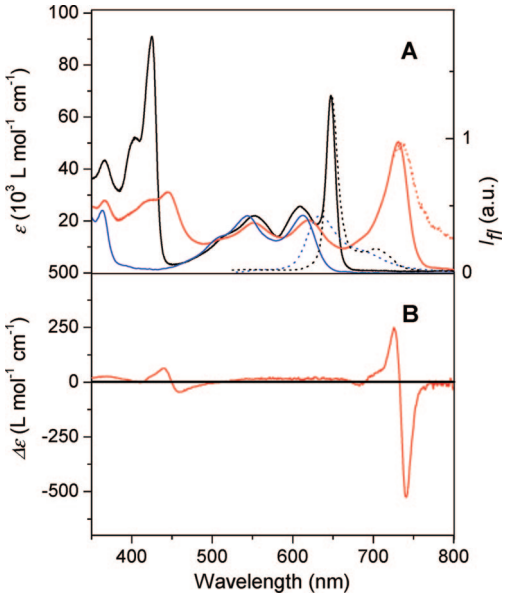

Figure 5. (A) UV–vis spectra (solid lines) and normalized fluorescence spectra (dotted lines) of triad **3** monomers in THF (black, $\lambda_{ex} = 510$ nm) and of triad **3** aggregates (red, $\lambda_{ex} = 540$ nm) and NDI_{NN}-NDI_{NO} **18** (blue, $\lambda_{ex} = 520$ nm) in cyclohexane/tetrachloromethane (1%). (B) CD spectrum of triad **3** aggregates in cyclohexane/tetrachloromethane (1%) (red).

conclusion that the ZnChl aggregates formed in cyclohexane/tetrachloromethane (1%) from ZnChl-NDI dyads **1**, **2** and from triad **3** are of a similar type, although the bulkier NDI_{NN}-NDI_{NO} functionalities at the periphery of **3** aggregates appear to be more impedimental toward rod formation than the NDI units at the circumference of **1** and **2** aggregates.

Time-Resolved Fluorescence Measurements. The elevation of the LH capacity of **1**–**3** aggregates by peripheral NDI chromophores depends on the efficiency of energy transfer from these NDI units to the ZnChl rod antenna. Stationary fluorescence spectroscopy suggests that complete energy-transfer quenching of the NDI units takes place in both the monomers and the aggregates (*vide supra*). To gain more insight into the excited-state properties of the monomeric compounds **1**–**3**, time-resolved fluorescence studies were carried out using 2-methyltetrahydrofuran as a solvent by the single photon timing technique for various excitation wavelengths and the results were analyzed by global analysis.[17]

Table 1. Fluorescence Lifetimes and Corresponding Amplitudes at Indicated Wavelengths for Monomers of Dyads **1** and **2** in 2-Methyltetrahydrofuran

ZnChl-NDI_{NO} **1** ($\lambda_{ex} = 540$ nm)			ZnChl-NDI_{NN} **2** ($\lambda_{ex} = 620$ nm)		
	amplitudes[a]			amplitudes[a]	
τ	@ 575 nm	@ 650 nm	τ	@ 625 nm	@ 655 nm
13 ns	0.30	0.14	12 ns	0.10	0.22
0.85 ns	0.15	4.3	0.14 ns	0.22	3.7
160 ps	0.35	0.58	75 ps	0.27	0.40
25 ps[b]	1.4	−2.0	7 ps[b]	2.2	−4.1

[a] Negative amplitudes indicate rise components. [b] Predominant energy transfer component.

Table 2. Fluorescence Lifetimes for Reference Chromophores NDI_{NO} **4**, NDI_{NN} **5**, and ZnChl **6b** Monomers and Aggregates

compd	λ_{ex} (nm)	τ_1	τ_2	τ_3
NDI_{NO} **4**[a]	540	12 ns	-	-
NDI_{NN} **5**[a]	620	10 ns	-	-
ZnChl **6b** mon.[b]	640	4 ns	-	-
ZnChl **6b** agg.[c]	720	13 ps	45 ps	131 ps

[a] Cyclohexane/tetrachloromethane (1%). [b] 2-Methyltetrahydrofuran/methanol (1%). [c] *n*-Hexane/2-methyltetrahydrofuran (1%).

The results for dyads **1** and **2** are summarized in Table 1 (see Table 2 for lifetimes of the pure reference compounds), and the corresponding figures for the time-resolved data are given in the Supporting Information (Figure S4). The data show that ultrafast energy transfer with predominant amplitudes for lifetimes of 25 ps (for **1**) and 7 ps (for **2**) takes place in these monomeric units. Very small amplitudes of longer lifetimes (ca. 100 ps) reflect less efficiently transferring conformations.

For the examination of excited-state properties of triad **3** monomers, at first, predominantly the NDI_{NO} (and slightly the NDI_{NN}) units were excited with 540 nm ps laser pulses (Table 3 and Figure S5 in the Supporting Information). Again a highly efficient energy transfer takes place with a lifetime of $\tau = 22$ ps in the emission region of NDI_{NO}, while the contribution of the amplitude component of unquenched NDI_{NO} ($\tau = 8.0$ ns) is negligibly small. Evidence for a direct energy-transfer process, instead of a sequential process via the middle NDI_{NN} chromophore, is obtained from the time-resolved fluorescence measurements of the NDI_{NN}-NDI_{NO} reference compound **18** in 2-methyltetrahydrofuran. Excitation of **18** at 540 nm provided a 29 ps lifetime

(17) O'Connor, D. V.; Phillips, D. *Time-correlated single photon counting*; Academic Press: London, 1988.

Table 3. Fluorescence Lifetimes and Corresponding Amplitudes at Indicated Wavelengths for Monomers of Triad **3** in 2-Methyltetrahydrofuran

triad **3** (λ_{ex} = 540 nm)			triad **3** (λ_{ex} = 621 nm)		
	amplitudes			amplitudes	
τ	@ 575 nm	@ 650 nm	τ	@ 629 nm	@ 655 nm
8.0 ns	0	0.46	7.8 ns	0.06	0.09
2.0 ns	0.01	7.7	2.0 ns	0.26	3.4
150 ps	0.09	0.58	200 ps	0.25	0.69
22 ps[a]	1.5	−4.6	8 ps[a]	3.2	−3.9

[a] Dominant energy transfer component.

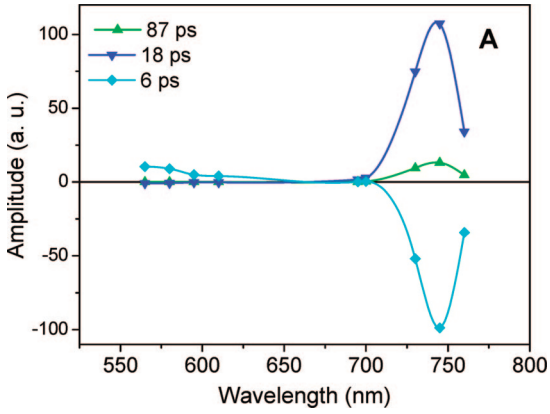

Figure 6. Fluorescence decay-associated spectra of aggregates of ZnChl-NDI_{NO} **1** (λ_{ex} = 540 nm; $c \approx 7.5 \times 10^{-6}$ M) in cyclohexane/tetrachloromethane (1%).

component, which turns from positive amplitude values in the wavelength range of the NDI_{NO} emission (λ < 620 nm) to negative amplitudes in the NDI_{NN} emission region (λ > 620 nm), indicating intramolecular energy transfer from NDI_{NO} to NDI_{NN} (for decay-associated spectra of **18**, see the Supporting Information, Figure S2). Thus, the time constant of FRET between NDI_{NO} and NDI_{NN} in **18** (τ = 29 ps) exceeds the time constant of the energy transfer observed for triad **3** (τ = 22 ps). Accordingly, in triad **3** the faster energy-transfer process is the direct transfer from NDI_{NO} to the ZnChl dye.

In a further experiment 621 nm excitation was used to excite directly the NDI_{NN} chromophore (Figure S5 in Supporting Information and Table 3). The main negative amplitude component (τ = 8 ps) indicates that highly efficient energy transfer from the NDI_{NN} units to the ZnChl chromophores takes place.

Time-Resolved Fluorescence of Aggregate Solutions of 1–3. To investigate the energy-transfer processes in self-assembled multichromophoric compounds **1**–**3**, time-resolved fluorescence measurements were conducted in cyclohexane/tetrachloromethane (1%) solutions. The NDI_{NO} unit of dyad **1** aggregates was excited with 540 nm laser pulses, which resulted in one dominant positive amplitude component with the lifetime τ = 6 ps in the wavelength region of the NDI_{NO} emission (λ < 640 nm) (Figure 6 and Table 4). The 6 ps amplitude component is negative in the emission region of ZnChl aggregates (λ > 700 nm), demonstrating that an ultrafast energy transfer from the NDI_{NO} chromophores to the self-assembled ZnChl aggregate takes place. Two positive amplitude components with lifetimes τ = 87 and 18 ps match the emission spectrum of the ZnChl **6b** aggregates (Table 2), reflecting the decay of those excited states that are generated by energy transfer from excited NDI_{NO} dyes. Multiexponential fluorescence decay is a typical feature

Table 4. Fluorescence Lifetimes and Corresponding Amplitudes at Indicated Wavelengths for Aggregates of ZnChl-NDI **1** and **2**[11] in Cyclohexane/Tetrachloromethane (1%)[a]

ZnChl-NDI_{NO} **1** (λ_{ex} = 540 nm)			ZnChl-NDI_{NN} **2** (λ_{ex} = 620 nm)		
	amplitudes			amplitudes	
τ	@ 560 nm	@ 745 nm	τ	@ 625 nm	@ 740 nm
10 ns	0.15	0.01	12 ns	0.09	0
87 ps	0.03	13	88 ps	0	2.9
18 ps	−0.86	108	18 ps	0	11
6 ps	11	−99	5 ps	0.69	−15

[a] Note that the nearly negligible amplitudes of the longer lifetimes are not shown in Figure 6 for the reason of better clarity.

of ZnChl rod aggregates, since for aggregates of ZnChl reference compound **6b** (see Table 2) and for natural BChl aggregates multiexponential decay characteristics have also been observed.[8] Furthermore, it had been reported earlier for ZnChl self-assemblies without appended dyes in L-α-Lecithin vesicles that the shortest lifetime component of the multiexponential decay is due to energy-transfer processes between different excitonic levels of the aggregate characterized by different radiative lifetimes.[8b] The other short lifetime components (<100 ps) are provoked by small amounts of oxidized chlorin that act as energy traps in model systems as well as in intact chlorosomes.[8b] These quenching processes are responsible for the generally low fluorescence quantum yields of ZnChl aggregates (*vide supra*).

Time-resolved fluorescence spectroscopic measurements on aggregates of ZnChl-NDI_{NN} **2** were performed before,[11] and for comparison, the results are listed in Table 4. As for dyad **1**, nearly complete quenching of the excited NDI_{NN} chromophores (λ_{ex} = 620 nm) has been observed for **2** and the dominant amplitude component (τ = 5 ps) in the short wavelength region turns strongly negative in the emission region of ZnChl aggregates (λ > 700 nm), indicating fast energy transfer. The lifetimes of the multiexponential ZnChl aggregate decay (18 and 88 ps) match the decay characteristics of dyad **1** aggregates.

Prior to investigating the photophysical processes in triad **3** aggregates, we have examined a solution of the NDI_{NN}-NDI_{NO} reference compound **18** in cyclohexane/tetrachloromethane (1%). Clear evidence for FRET from the excited NDI_{NO} chromophore to the NDI_{NN} unit in this solvent system has already been obtained from the steady-state emission spectrum of **18**, as only an emission band of NDI_{NN} has been detected (Figure 5A). To gain insight into the kinetics of this process, NDI_{NN}-NDI_{NO} **18** was irradiated with 540 nm laser pulses and the fluorescence decay was recorded in the range 575–680 nm (decay-associated spectra are shown in Figure S3). Global analysis revealed a 15 ps lifetime component, which turns from positive amplitudes in the wavelength region of the NDI_{NO} emission region (λ < 615 nm) to negative amplitudes in the NDI_{NN} emission region. This lifetime component is attributed to the energy transfer from NDI_{NO} to the blue NDI_{NN} dye.

The excited-state properties of triad **3** aggregates in cyclohexane/tetrachloromethane (1%) have been first investigated by exciting mainly the NDI_{NO} (and slightly NDI_{NN}) units at 540 nm. The resulting amplitude decay-associated (DAS) results are depicted in Figure 7A, and the amplitude components and their lifetimes are collected in Table 5. The spectrum of the component with lifetime τ = 6 ps in the short wavelength range ($\lambda \leq$ 700 nm) is characteristic for an efficient energy-transfer process from NDI_{NO} to the ZnChl antenna. A time constant of 6 ps for this process is considerably smaller than that observed for the energy transfer from NDI_{NO} to NDI_{NN} in reference

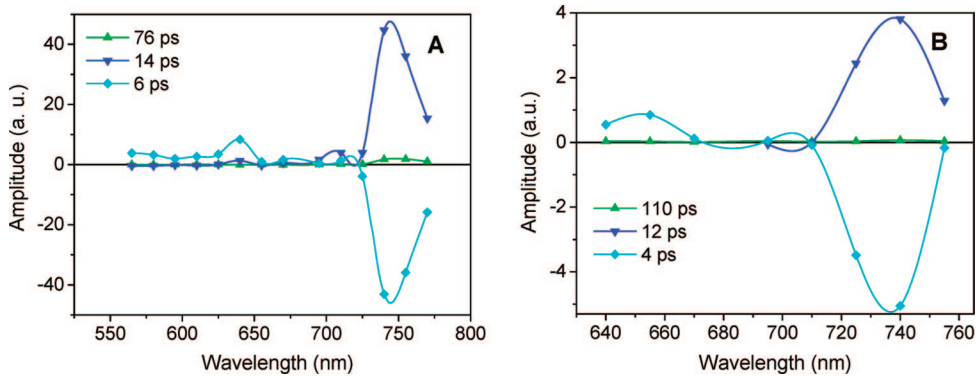

Figure 7. Fluorescence decay-associated spectra of aggregates of triad **3** in cyclohexane/tetrachloromethane (1%). (A) $\lambda_{ex} = 540$ nm; $c \approx 6.9 \times 10^{-6}$ M; (B) $\lambda_{ex} = 621$ nm; $c \approx 7.9 \times 10^{-6}$ M.

Table 5. Fluorescence Lifetimes and Corresponding Amplitudes at Indicated Wavelengths for Aggregates of Triad **3** in Cyclohexane/Tetrachloromethane (1%)[a]

triad **3** ($\lambda_{ex} = 540$ nm)				triad **3** ($\lambda_{ex} = 621$ nm)		
	amplitudes				amplitudes	
τ	@ 565 nm	@ 640 nm	@ 740 nm	τ	@ 640 nm	@ 740 nm
10 ns	0.02	0.69	0.12	10 ns	0.14	0
76 ps	0.02	−0.10	1.8	110 ps	0.03	0.06
14 ps	−0.39	1.3	47	12 ps	0	3.4
6 ps	3.8	8.4	−43	4 ps	0.49	−4.5

[a] Note that the nearly negligible amplitudes of the longer lifetimes are not shown in Figure 7 for the reason of better clarity.

compound **18** ($\tau = 15$ ps). Thus, upon excitation of NDI_{NO} in triad **3** the excitation energy is directly transmitted, at least in part, to the ZnChl antenna rather than being transferred along a cascade via the NDI_{NN} unit. The decay of the excited ZnChl aggregate, which is generated by this energy transfer, shows again the characteristic multiexponential behavior with a major 14 ps and a minor 76 ps amplitude component.

In a further experiment, 621 nm laser pulses were chosen to excite the NDI_{NN} unit (Figure 7B and Table 5). The large positive amplitude of a $\tau = 4$ ps component in the NDI_{NN} emission region (wavelengths $\lambda \leq 670$ nm) turns negative in the ZnChl aggregate emission ($\lambda \geq 710$ nm) region and can, therefore, be assigned to the fast energy-transfer process from NDI_{NN} chromophores to the ZnChl rod antenna. The multiexponential decay of ZnChl aggregates is dominated by a 12 ps lifetime component and a few additional longer wavelength components with much smaller amplitudes.

The decay pathways that followed after excitation of the respective NDI units in **1**−**3** aggregates are illustrated in energy-level diagrams shown in Figure 8. The energy-level diagram and photophysical processes of triad **3** aggregates nearly resemble the sum of the diagrams of dyads **1** and **2**. The most remarkable feature in triad **3** is the ultrafast energy transfer, directly from the outer red NDI unit to the central ZnChl rod aggregate.

Light-Harvesting Efficiencies. The singlet–singlet excitation energy-transfer efficiencies from NDI to ZnChl chromophores in **1**–**3** monomers and ZnChl rod antenna aggregates can in principle be estimated either from steady-state or from time-resolved fluorescence data. To calculate energy-transfer efficiencies from steady-state spectroscopic measurements, it is necessary to record excitation spectra at an acceptor emission wavelength which is separated from the donor emission region. However, for monomers of **1**−**3**, it was not possible to find an appropriate detection wavelength, since the broad S_0-S_1 emission band of NDI_{NO} and NDI_{NN}, respectively, overlaps with the rather narrow emission band of the ZnChl monomer. Therefore, all the recorded excitation spectra of **1**–**3** monomers did not exactly match with the respective absorption spectrum but showed a too small contribution of the ZnChl band. Moreover, the fluorescence intensities of **1**−**3** aggregates are too low to obtain excitation spectra of these species that would be suitable for a quantitative analysis. Hence, we decided to calculate energy-transfer efficiencies from time-resolved data by using the following relationship:

$$\phi_{ET} = \frac{k_{ET}}{k_{ET} + k_D}; \; k = \frac{1}{\tau} \qquad (1)$$

where ϕ_{ET} is the energy-transfer efficiency, k_{ET} is the energy-transfer rate, and k_D is the donor fluorescence decay rate in the absence of the acceptor. Values for k_{ET} and k_D can be easily calculated from the respective lifetimes that have been obtained from spectroscopic measurements.

The resulting values are summarized in Table 6. The energy-transfer rates for **1**−**3** monomers are calculated to be in the range $(4.0–4.5) \times 10^{10}$ s^{-1} if NDI_{NO} acts as an energy donor and $(1.3–1.4) \times 10^{11}$ s^{-1} with NDI_{NN} as the donor unit. Energy-transfer rates from peripheral NDI chromophores to the ZnChl rod aggregate are even larger showing values of 1.7×10^{11} s^{-1} at excitation of the NDI_{NO} chromophore and $(2.0–2.5) \times 10^{11}$ s^{-1} when NDI_{NN} units are excited. Energy-transfer processes from NDI_{NN} donors are slightly faster than those from NDI_{NO} units for both **1**−**3** monomers and aggregates, which can be related to the larger overlap integral of the NDI_{NN} emission spectrum with the ZnChl monomer or aggregate absorption spectrum compared to the respective overlap area observed for ZnChl-NDI_{NO}. Due to the high energy-transfer rates, we obtained energy-transfer efficiencies of $\phi_{ET} \geq 99\%$ for monomers as well as for aggregates of **1**–**3**.

As we have shown that all excited NDI units transfer their energy directly and completely to the ZnChl rod, the increase of the sunlight harvesting capacity of the multichromophoric LH systems **1**−**3**compared to the monochromophoric aggregates of reference system ZnChl **6a** can be calculated from the ratio of the respective cross sections of terrestrial solar light absorption. For aggregates of dyad ZnChl-NDI_{NN} **2**, an increase of 26% of the total LH efficiency lent by appended NDI dyes was calculated.[11,18] For the new dyad ZnChl-NDI_{NO} **1**, an improvement to 36% is reached,

(18) The cross sections can be calculated by integration of the products of the respective absorption values and the terrestrial solar irradiance (for details, see the Supporting Information).

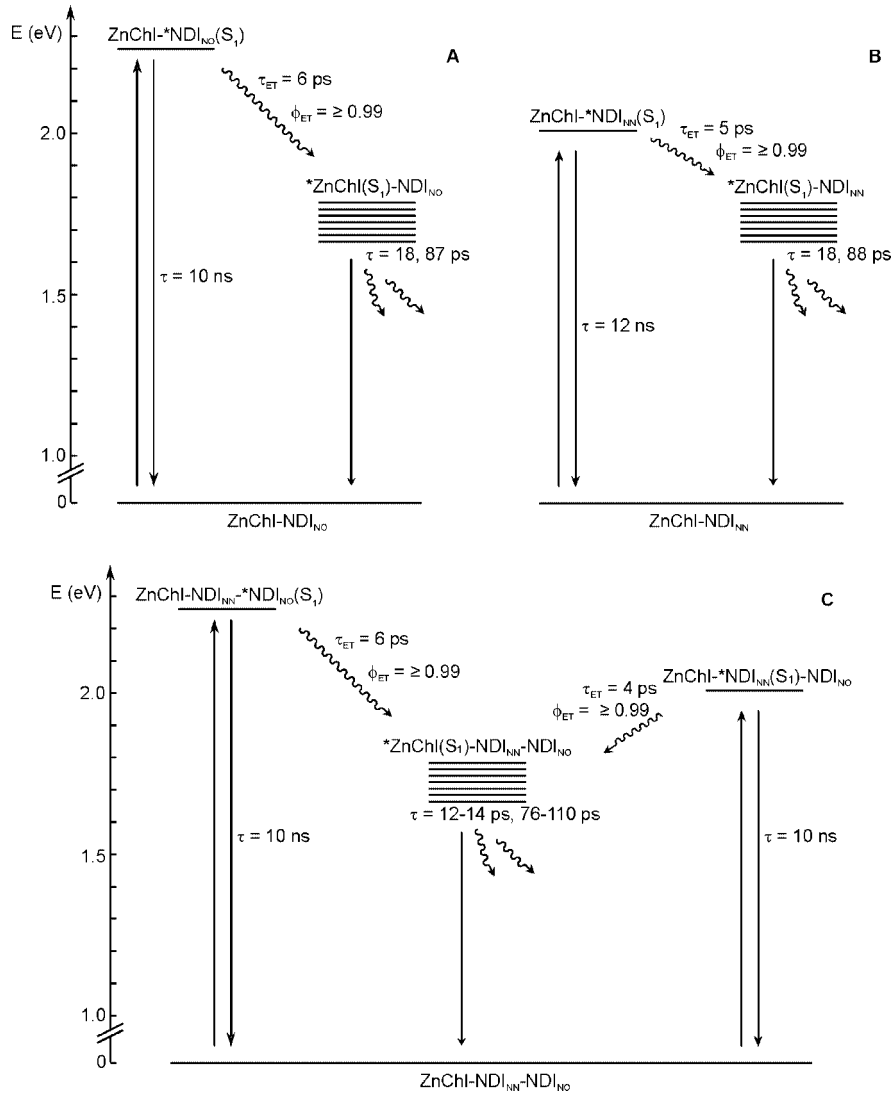

Figure 8. Energy-level diagram and photophysical behavior of aggregates of (A) ZnChl-NDI$_{NO}$ **1**, (B) ZnChl-NDI$_{NN}$ **2**, and (C) ZnChl-NDI$_{NN}$-NDI$_{NO}$ **3** in cyclohexane/tetrachloromethane (1%).

Table 6. Energy-Transfer Rates and Efficiencies for **1**−**3** Monomers in 2-Methyltetrahydrofuran and **1**–**3** Rod Aggregates in Cyclohexane/Tetrachloromethane (1%) Derived from Time-Resolved Emission Data

	monomers				aggregates			
	k_D				k_D			
compd	NDI$_{NO}$ (s^{-1})	NDI$_{NN}$ (s^{-1})	k_{ET} (s^{-1})	ϕ_{ET} (%)	NDI$_{NO}$ (s^{-1})	NDI$_{NN}$ (s^{-1})	k_{ET} (s^{-1})	ϕ_{ET} (%)
1	7.7×10^7		4.0×10^{10}	≥99	1.0×10^8		1.7×10^{11}	≥99
2		8.3×10^7	1.4×10^{11}	≥99		9.1×10^7	2.0×10^{11}	≥99
3	1.3×10^8		4.5×10^{10}	≥99	1.0×10^8		1.7×10^{11}	≥99
3		1.3×10^8	1.3×10^{11}	≥99		1.0×10^8	2.5×10^{11}	≥99

and the best result is achieved for triad **3** revealing an increase of 63% of the total LH efficiency.

Conclusions

We have demonstrated that it is possible to equip the biomimetic ZnChl rod antennae with additional peripheral LH chromophores, without the assistance of a structure-stabilizing protein matrix. This goal has been achieved by self-assembly of multichromophoric arrays based on covalently linked ZnChl-NDI dyads **1**, **2** and, more pleasingly, with the triad ZnChl-NDI$_{NN}$-NDI$_{NO}$ **3** containing additional chromophores to cover the green and orange fractions of solar light. UV–vis, CD, and stationary fluorescence spectroscopy revealed that in nonpolar aprotic solvents such as cyclohexane/tetrachloromethane (1%) self-assembled ZnChl J-aggregates are formed by intermolecular interactions of ZnChl units of ZnChl-NDI conjugates **1**–**3**, whereas the appended NDI chromophores remain not aggregated at the periphery.

Time-resolved fluorescence experiments revealed that upon selective excitation of peripheral blue NDI$_{NN}$ or pink NDI$_{NO}$ units their excitation energy is conveyed quantitatively and directly to the inner green ZnChl rod antenna by highly efficient energy-transfer processes. Thus, the "green gap" can be efficiently covered by the attached NDI antenna chromophores, providing black dye aggregates whose sunlight harvesting

efficiency is increased by up to 63% compared to the parent ZnChl or natural BChl *c* rod aggregates.

Acknowledgment. C.R. is grateful to the Degussa Stiftung for a PhD scholarship. We thank the Fonds der Chemischen Industrie for financial support.

Supporting Information Available: Experimental information. This material is available free of charge via Internet at http://pubs.acs.org.

JA710253Q